Reverse Monte Carlo study of structure changes in amorphous $Pd_{52}Ni_{32}P_{16}$ upon annealing

Peter A. Duine, Jilt Sietsma, and Barend J. Thijsse
Laboratory of Materials Science, Delft University of Technology, Rotterdamseweg 137, 2628 AL Delft, The Netherlands

László Pusztai
L. Eötvös University, Budapest, Hungary

(Received 28 February 1994; revised manuscript received 28 July 1994)

Structure changes in amorphous $Pd_{52}Ni_{32}P_{16}$ upon relaxation were modeled by means of reverse Monte Carlo (RMC) simulations using neutron-diffraction data from M. Schaal, P. Lamparter, and S. Steeb [Z. Naturforsch. Teil A **43**, 1055 (1988)] as input for the RMC program. Two states after annealing (2 h at 570 K and 2 h at 607 K) and the as-quenched state were successfully modeled. The resulting three-dimensional models of the structure were inspected for changes in the nearest-neighbor coordinations (short-range order) and for changes at larger interatomic distances (medium-range order) upon relaxation. It was found that the short-range order is affected by annealing, resulting in, for instance, a sharpening of the Voronoi volume distribution. These results were found to agree with interpretations of experimental atomic mobility studies. The effect of annealing on multibody correlation functions for medium-range distances is much less pronounced than that for the short-range distances, and the two appear to be largely decoupled from one another. These results, together with the observed annealing effect on the decay rate of the peaks of the reduced radial distribution function, suggest that medium-range ordering is not merely a reflection of short-range ordering, but has its origin in a change in propagation of disorder in the structure. Medium-range ordering can therefore be treated as a separate effect of annealing.

I. INTRODUCTION

Changes in the structure of amorphous metals upon annealing can be observed with neutron and x-ray diffraction and the observed changes in the diffraction patterns have been used to model structural relaxation.[1,2] A detailed experimental study of structure changes upon annealing has been performed by Schaal, Lamparter, and Steeb[3] on amorphous $Pd_{52}Ni_{32}P_{16}$ using neutron diffraction and isotopic substitution. According to their analysis of the Ni-Ni distance distributions, structural relaxation in amorphous $Pd_{52}Ni_{32}P_{16}$ mainly involves a redistribution of bond angles, appearing as changes in the second distance shell, but leaves the nearest-neighbor distance distribution nearly unchanged. It is interesting to extend the analysis of Schaal, Lamparter, and Steeb to other nearest-neighbor correlations and study the effect of annealing on the structure of amorphous $Pd_{52}Ni_{32}P_{16}$ in more detail. Furthermore, it is interesting to compare the experimental diffraction results of Schaal, Lamparter, and Steeb to other quantities measured during structural relaxation. In particular, the question arises whether the explanations given for the reduction of atomic mobility in amorphous metals upon annealing are consistent with the experiments of Schaal, Lamparter, and Steeb. The interpretation of this effect usually involves a change in the nearest-neighbor environment, e.g., a reduction of localized defects, like free-volume fluctuations,[4] upon annealing. A realistic three-dimensional model of the structure of amorphous $Pd_{52}Ni_{32}P_{16}$ could clarify whether such interpretations of atomic mobility data are consistent with the above-mentioned diffraction experiments.

To overcome the limitations of the traditional methods employed by Schaal, Lamparter, and Steeb to analyze the diffraction data, we have performed an alternative analysis of their data by means of reverse Monte Carlo (RMC) simulations. The RMC technique originated with McGreevy and Pusztai,[5] who were the first to extract a three-dimensional model of liquid argon by simply fitting a set of atomic positions to the results of the diffraction experiment. Later, Pusztai,[6] Keen and McGreevy,[7] and Iparraguirre *et al.*[8] successfully applied this technique to metallic glasses. Not only are the *pair*-correlation functions of these models in good agreement with the diffraction experiment, but also *multibody* correlation functions (i.e., involving the positions of more than two atoms simultaneously) for the short-range distances, such as the cosine of bond angles, Voronoi volume, and nearest-neighbor distributions, agree with results of molecular dynamics and Monte Carlo simulations.[9] This is of particular importance, since it means that RMC models do give a complete picture of the characteristics of the structure under investigation. It is therefore expected that the present analysis will provide realistic distributions of the multibody correlation functions and, more importantly, the changes therein upon annealing.

The three-dimensional models also offer the possibility to investigate correlation functions over distances that correspond to the third, fourth, etc., peak of the pair-correlation function. We have chosen to study this effect of annealing separately from the effect on the short-range distances, since the data of Schaal, Lamparter, and Steeb[3] indicate that medium-range order is likely not solely brought about by short-range interactions (see Sec. II),

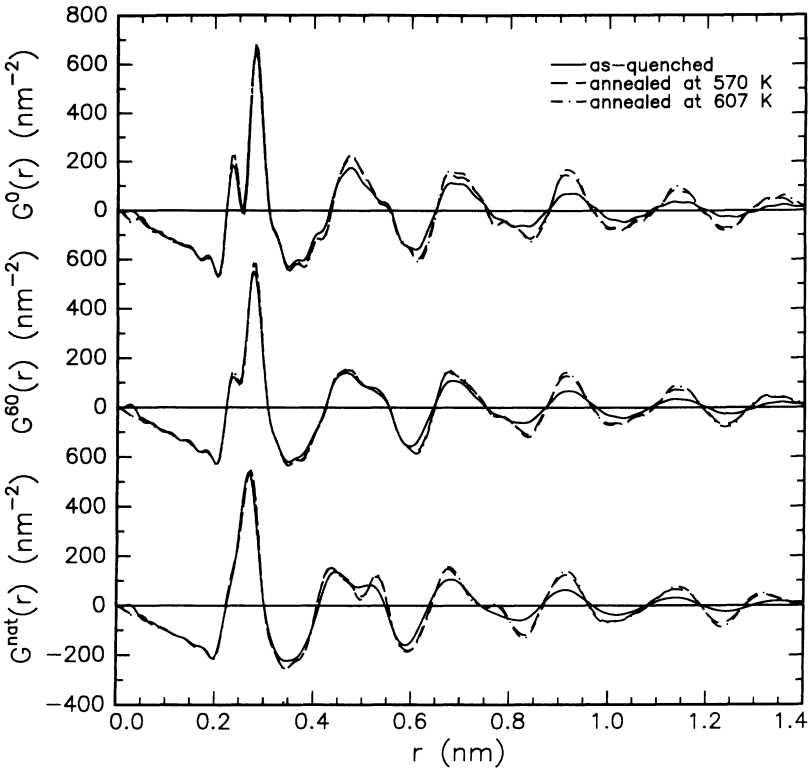

FIG. 1. Reduced radial distribution functions $G(r)$ for the three different samples in the as-quenched condition and after annealing for 2 h at 570 and at 607 K. $G^{nat}(r)$ refers to a sample with the natural isotope composition of Ni, $G^{60}(r)$ refers to a sample with the ^{60}Ni isotope, and $G^{0}(r)$ refers to a sample with a composition of ^{60}Ni and ^{62}Ni such that the resulting scattering length for Ni is zero (Ref. 3).

but has to be treated as a separate characteristic of the structure. This conjecture is corroborated by empirical studies of radial distribution functions of several metallic glasses,[10,11] and by the general conception of the glass formation as being a competition between short- and medium-range order. More details on the calculations of this RMC study have been reported in Ref. 12.

II. THE DATA

Schaal, Lamparter, and Steeb[3] performed a neutron-diffraction study on three different samples of amorphous, melt-quenched $Pd_{52}Ni_{32}P_{16}$, composed with ^{nat}Ni, ^{60}Ni, and with a mixture of the ^{60}Ni and ^{62}Ni isotopes, having a zero scattering length (^{0}Ni). The three data sets that were used as input for the RMC programs are presented in Fig. 1 as reduced radial distribution functions $G(r)$,

$$G(r)=\frac{2}{\pi}\int_0^\infty Q[S(Q)-1]\sin(Qr)dQ \ , \tag{1}$$

with $S(Q)$ the well-known structure factor, and r the interatomic distance. $S(Q)$ was measured over the range 3–160 nm^{-1} for the momentum transfer Q. In a multicomponent metallic glass, $G(r)$ is given by the sum of the partial reduced radial distribution functions:

$$G(r)=\sum_i\sum_j W_{ij}G_{ij}(r) \ , \tag{2}$$

with W_{ij} the weighting factors. Table I gives the weighting factors for the three data sets (reproduced from Ref. 3). The partial reduced radial distribution function $G_{ij}(r)$ is related to the partial number density $\rho_{ij}(r)$ of j-type atoms at a distance r from an i atom by

$$G_{ij}(r)=4\pi r\left[\frac{\rho_{ij}(r)}{c_j}-\rho_0\right] \ , \tag{3}$$

with ρ_0 the average number density and c_j the molar fraction of component j. A related function is

$$g_{ij}(r)=\frac{\rho_{ij}(r)}{c_j\rho_0} \ , \tag{4}$$

which is called the partial pair-correlation function. The total pair-correlation function is given by the sum of the partial pair-correlation functions [analogous to Eq. (2)].

Clearly, Fig. 1 shows that annealing for 2 h at 570 K results in a $G(r)$ similar to that after annealing for 2 h at 607 K, both quite different from the as-quenched $G(r)$. This makes this data set suited for a model study of structure changes upon annealing, since we expect to find structural differences between models of the as-quenched and annealed structures, and negligibly small differences (i.e., only arising from statistical fluctuations) between models representing the structure of amorphous $Pd_{52}Ni_{32}P_{16}$ after annealing at 570 and 607 K. In this

TABLE I. Neutron-diffraction weighting factors for the Pd^{nat}NiP, Pd^{60}NiP, and Pd^{0}NiP samples.

Sample	$W_{Pd\text{-}Pd}$	$W_{Pd\text{-}Ni}$	$W_{Pd\text{-}P}$	$W_{Ni\text{-}Ni}$	$W_{Ni\text{-}P}$	$W_{P\text{-}P}$
Pd^{nat}NiP	0.183	0.392	0.098	0.210	0.105	0.013
Pd^{60}NiP	0.412	0.240	0.220	0.035	0.064	0.029
Pd^{0}NiP	0.623	0.000	0.333	0.000	0.000	0.044

way, the two annealed structures offer an indication of the uncertainties in the results.

It appears from Fig. 1 that the higher-order coordination shells are much more affected by annealing than the first coordination shell. However, changes in the first coordination shell do occur and they can be characterized, for instance, by the Wendt-Abraham parameter $\mathcal{R}^{(1)}$ (Ref. 13) according to

$$\mathcal{R}^{(k)}=\frac{g_{\min}^{(k)}}{g_{\max}^{(k)}}\ , \tag{5}$$

with $g_{\min}^{(k)}$ and $g_{\max}^{(k)}$ the values of the pair-correlation function at the kth minimum (not counting the minimum at $r=0.2$ nm) and the kth maximum, respectively. The Wendt-Abraham parameters for $k=1$ are given in Fig. 2 and indicate that the nearest-neighbor distances in the as-quenched structure are more dispersed than in the structures after annealing. Both annealing treatments result in roughly the same $\mathcal{R}^{(1)}$.

To investigate the effect of annealing more precisely, we plot in Fig. 3 for the natural Ni sample the difference in the pair-correlation functions $\Delta g(r)$,

$$\Delta g(r)=g_{\rm an}(r)-g_{\rm aq}(r)\ , \tag{6}$$

with $g_{\rm an}(r)$ and $g_{\rm aq}(r)$ the total pair-correlation functions of the annealed and the as-quenched sample, respectively. In $\Delta g(r)$ one observes that, upon annealing, the first peak in $g(r)$ shifts to a higher value of r (visible in the strong oscillations for 0.2 nm $<r<$ 0.3 nm), almost without becoming sharper (Fig. 1), and the other minima and maxima in $g(r)$ become sharper without shifting along the r axis. The difference in behavior of the first peak and the higher-order peaks suggests that the changes in the higher-order coordination shells are not merely a reflection of the changes taking place in the first coordination shell.[14] It is more likely that the changes in the higher-order coordination shells also involve changes in the diffusive propagation of order in the structure, i.e., in the way in which local environments interconnect. This can be investigated by calculation of the decay rate of the peak heights of the reduced radial distribution function

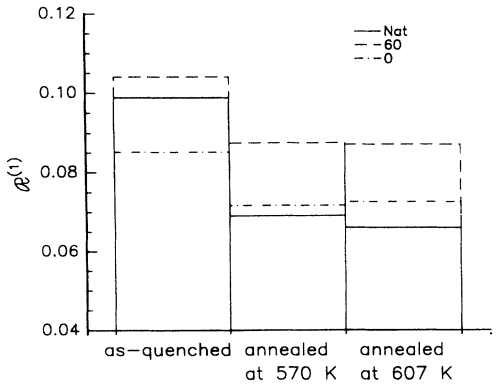

FIG. 2. Wendt-Abraham parameters $\mathcal{R}^{(1)}$ [see Eq. (5)] for the three different samples in the as-quenched condition and after annealing at 570 and 607 K.

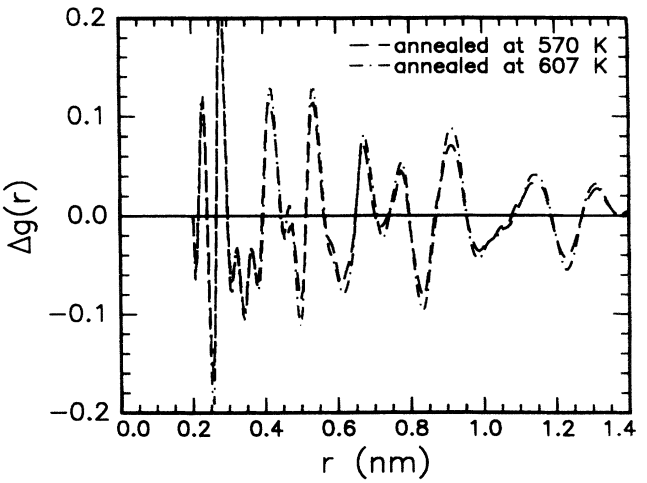

FIG. 3. The differences in the pair-correlation functions for the natural Ni sample in the as-quenched state and after annealing at 570 and 607 K [see Eq. (6)].

$G(r)$. It has been shown[11] that the peak heights of quite a number of metallic glasses decay approximately exponentially with $r_*^{(k)}$ according to

$$G(r^{(k)})=\alpha\exp(-\beta r_*^{(k)})\ , \tag{7}$$

with α a constant, $r_*^{(k)}$ the normalized peak position of the kth peak ($r_*^{(k)}=r^{(k)}/r^{(1)}$), and β the decay rate, which is considered a measure of the diffusive propagation of order in the structure. Figure 4 shows, in agreement with

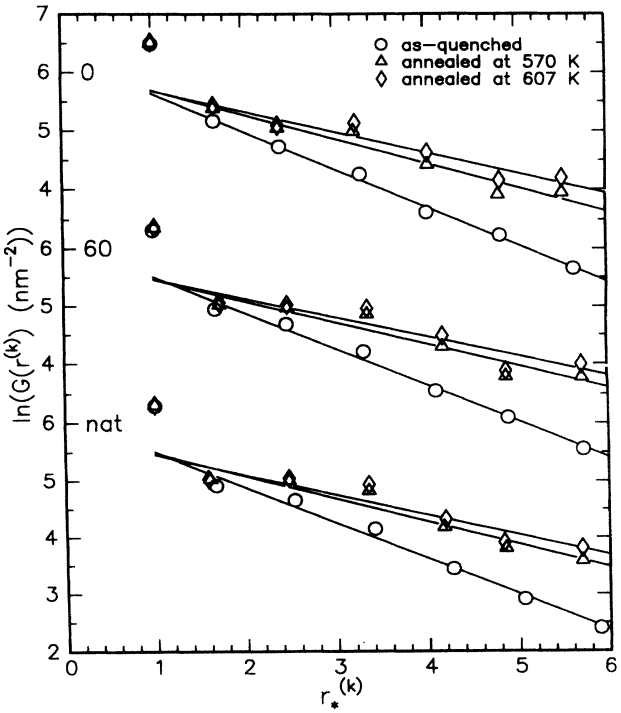

FIG. 4. Logarithm of the maxima $G(r^{(k)})$ versus normalized peak position $r_*^{(k)}$ for the three different samples in the as-quenched and annealed conditions.

what is found for other metallic glasses,[10,11] that the height of the first peak does not fit into this exponential decay model, but that the decay from the second to the seventh peak is roughly exponential. The decay rate β shows a pronounced reduction upon annealing (from 0.63 ± 0.02 for the as-quenched samples to 0.39 ± 0.02 and 0.34 ± 0.01 for the samples annealed at 570 and 607 K, respectively). This reduction of β is considerably larger than observed for other metallic glasses upon annealing[11] and it covers the major effect of annealing on the medium range order of amorphous $Pd_{52}Ni_{32}P_{16}$. It suggests that the changes in the medium-range order upon annealing originate from changes in the propagation of order in the structure, rather than being directly related to changes in short-range order. This consideration makes it still more unlikely that the effect of annealing at medium-range distances is solely the result of the sharpening of the short-range order.

III. RMC PROCEDURES

In general, reverse Monte Carlo calculations are carried out by randomly picking an atom of a three-dimensional model of the structure, moving the atom in a random direction, and comparing the pair distances of the new model with the diffraction data.[5] If the model shows a better agreement than before, the displacement is accepted; if not, the displacement is accepted with a certain probability which prevents the configuration of being trapped in a local minimum. The calculation is completed once a measure of the goodness of fit reaches a minimum. Further details and a review of the method can be found in Ref. 15.

Ideally, a study of the structure of a three-component metallic glass would require six independent measurements with considerably different weighting factors as input for the Reverse Monte Carlo simulation. Nevertheless, just as in a recently reported case for a binary glass with two experimental functions,[16] the present RMC simulation of a ternary glass using only three experimental functions yields consistent and meaningful results. Besides experimental diffraction data, knowledge of the density of the amorphous samples is of importance for the construction of an RMC model of the structure of amorphous $Pd_{52}Ni_{32}P_{16}$. However, the density of the samples was not exactly known, and we have therefore calculated the density on the basis of the scaling relations of the density reported for metallic glasses.[17] This resulted in a density of 75.0 atoms/nm^3, i.e., 9.26 g/cm^3. This density is slightly lower than the density determined from the diffraction data (^{0}Ni sample $\rho_0=85$, ^{60}Ni sample $\rho_0=80$, and natural Ni sample $\rho_0=78$ atoms/nm^3). However, RMC test runs at $\rho_0=80$ atoms/nm^3 did not result in an acceptable fit to the diffraction data.[12] Furthermore, although it was realized that the density of an amorphous metal typically increases 0.2% upon annealing (this value was found for amorphous $Pd_{40}Ni_{40}P_{20}$ as measured by the Archimedes method;[2] the detection limit by diffraction corresponds to a much larger density change[18]), all the simulations were carried out with $\rho_0=75$ atoms/nm^3, since the density change was considered too small to be important.

Our simulations started with the production of a hard-sphere packing of 266 Pd, 164 Ni, and 82 P atoms in a cubic box of 6.827 nm^3. Explicit values for the closest approach distances (Δ_{ij}) were determined by carrying out test runs, which resulted in $\Delta_{Pd\text{-}Pd}=0.25$ nm, $\Delta_{Pd\text{-}Ni}=0.22$ nm, $\Delta_{Pd\text{-}P}=0.21$ nm, $\Delta_{Ni\text{-}Ni}=0.24$ nm, $\Delta_{Ni\text{-}P}=0.21$ nm, and $\Delta_{P\text{-}P}=0.30$ nm.[12] Subsequently, reverse Monte Carlo simulations were carried out with periodic boundary conditions and the three measured pair-correlation functions as input for the RMC program. This was done for the three as-quenched pair-correlation functions as well as for the two data sets taken after annealing. Upon reaching the best fit, the edge length of the simulation box was doubled to 3.794 nm, resulting in a volume of 54.613 nm^3 containing 4096 particles. After further RMC calculations satisfactory fits were reached. Visual inspection of the three-dimensional models showed some remnants of the original simulation box size, but this spurious quasiperiodicity did not show up in the calculations of multibody correlation functions. The above procedure resulted in three models [hereafter designated as $g(r)$ models] of the structure of amorphous $Pd_{52}Ni_{32}P_{16}$, different from each other only because of the difference in the pair-correlation functions of the as-quenched and annealed samples. Figure 5 gives a schematic representation of the models obtained in this study; the $g(r)$ models are shown in the second row.

In order to investigate the influence of the *type* of fitting function for the reverse Monte Carlo simulation, additional calculations were carried out where we used $G(r)$, $S(Q)$, and $\Gamma(r)$ as input for the RMC program. $\Gamma(r)$ is defined by $\Gamma(r)=G(r)/|G|$,[8] where $|G|$ denotes the average over r of the absolute value of $G(r)$, and was chosen to account for the uncertainty in the normalization of the measured diffraction intensities. In the case of

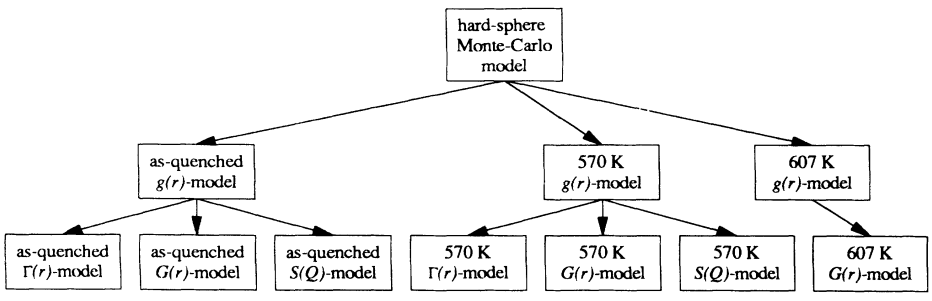

FIG. 5. Generation scheme of the models of the structure of amorphous $Pd_{52}Ni_{32}P_{16}$.

$Ni_{81}B_{19}$ studied by Iparraguirre *et al.*,[8] the renormalization factors proved to be a rather substantial 1.05 to 1.20, in the present case the normalization corrections were roughly 1.08, i.e., the experimental $|G|$ were 8% too large. This explains why the density calculated from the diffraction data is (roughly 7%) too high.

These additional runs were carried out with the $g(r)$ models rather than the hard-sphere packing as starting model (see the third row of Fig. 5). This implies that the resulting models [hereafter designated as $G(r)$ models, $S(Q)$ models, and $\Gamma(r)$ models] are not truly independent of one another, but reflect the structural differences resulting from the (rather arbitrary) choice of input data. It will be shown that these differences are smaller than the differences in the structure resulting from the annealing treatment.

IV. RESULTS

An indication of the fit quality of the model calculations (see Fig. 5) is given in Fig. 6, where $G(r)$ models are shown for the as-quenched and annealed samples with the ^{0}Ni composition. Clearly, the $G(r)$ models agree very well with the experimental data, and, in particular, the changes in the experimental $G(r)$ upon annealing are well reproduced. Table II gives E^2 values {with $E^2=(1/N)\sum_1^N[G_{\text{calc}}(r)-G_{\text{meas}}(r)]^2$ and N the number of data points} for $G(r)$ models of the structure of amorphous $Pd_{52}Ni_{32}P_{16}$. It is important to note that all fits are of similar quality, making spurious structure differences resulting from different fit qualities unlikely. The quality of the $g(r)$, $S(Q)$, and $\Gamma(r)$ models is similar.

Based on the weighting factors for the three different samples (Table I), the uncertainty in the P-P and Ni-P partial pair-correlation functions is much higher than in the other four and these will therefore not be discussed. Moreover, the Pd-P partial pair-correlation function shows a sharply split first peak,[12] which changes dramatically upon both the 570 and the 607 K annealing treatment. Such a big change seems to be an artefact of the limited input for the RMC program.

TABLE II. Fit qualities (E^2) for the $G(r)$ models.

Sample	as-quenched nm^{-4}	570 K nm^{-4}	607 K nm^{-4}
$Pd^{nat}NiP$	164	171	221
$Pd^{60}NiP$	155	123	113
$Pd^{0}NiP$	227	241	177

The three remaining partial pair-correlation functions (Pd-Pd, Pd-Ni, Ni-Ni) will be analyzed further in this work, and these partials are shown in Fig. 7. Upon annealing they behave similarly to the measured total $G(r)$'s, i.e., a small change in $\mathcal{R}^{(1)}$ and a considerable change in the decay rate β (roughly a reduction of 20%). To investigate the effect of annealing on the structure of amorphous $Pd_{52}Ni_{32}P_{16}$ in more detail, we have calculated multibody correlation functions for the short- and medium-range distances involving only metal-metal correlations. The results will be discussed in Sec. V.

V. DISCUSSION

A. Short-range order

We have characterized the short-range order in the models of the structure of amorphous $Pd_{52}Ni_{32}P_{16}$ by us-

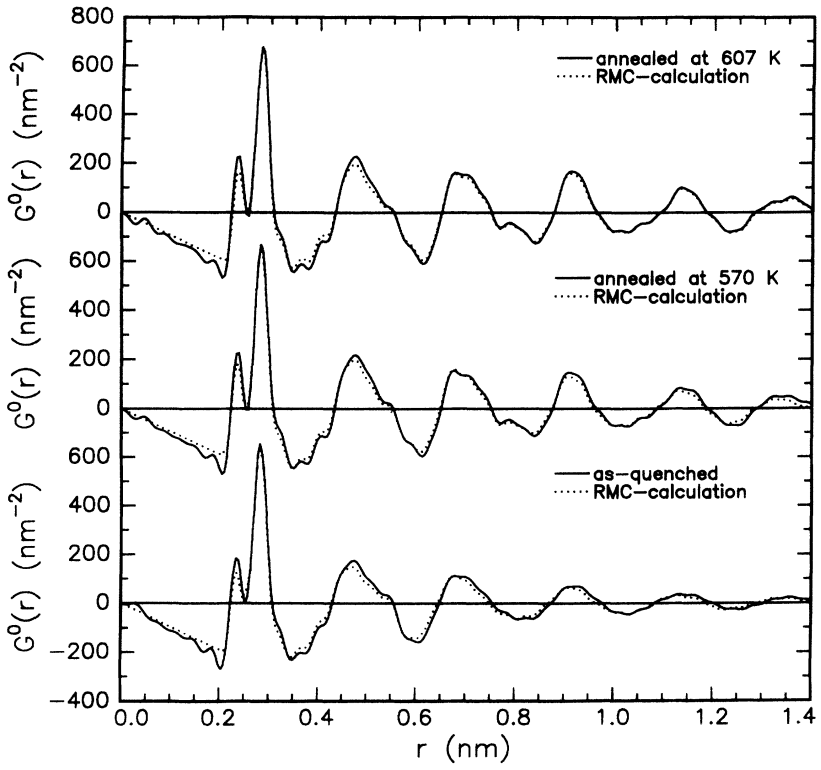

FIG. 6. $G(r)$ for three ^{0}Ni samples (as-quenched and annealed at 570 and 607 K), calculated (dotted lines) and measured (Ref. 3).

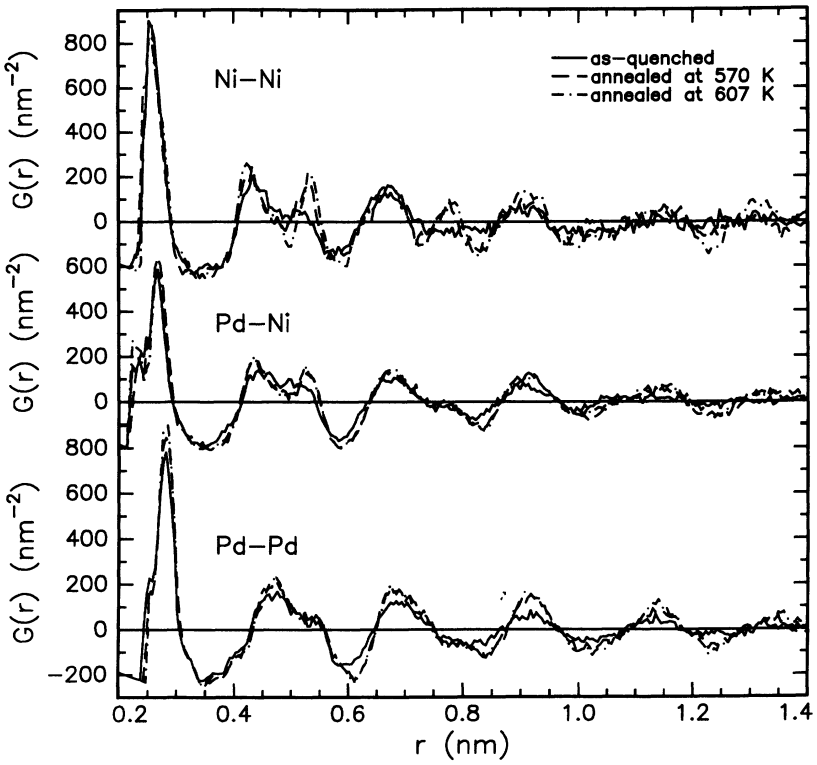

FIG. 7. $G_{\text{Pd-Pd}}(r)$, $G_{\text{Pd-Ni}}(r)$, and $G_{\text{Ni-Ni}}(r)$ for the $G(r)$ models of the as-quenched and annealed states.

ing various well-known tools for the structural analysis of nearest-neighbor topology. In general, nearest-neighbors are defined as atoms having pair distances smaller than 0.35 nm. Note that, as stated in the previous section, we will only consider metal-metal correlation functions.

In Fig. 8 the distribution of nearest Pd neighbors around Pd atoms in the $G(r)$ models of the as-quenched and annealed structures is given. It can be seen that the effect of annealing on the nearest-neighbor distribution is very small. Neighbor distributions calculated for Pd atoms in other models of the structure [e.g., $S(Q)$ models] are virtually identical to the ones shown in Fig. 8. Also the nearest-neighbor distributions of other elements show very small changes upon annealing.

The distribution of cosines of bond angles shows a more pronounced effect of annealing. Cosine distributions are three-atom correlation functions which can be calculated by defining a bond as the vector joining two neighboring atoms. The cosine is taken of the angle θ between the two bonds of a triplet of atoms. Figure 9 shows the distribution of cosines of the angle θ between the two bonds of Pd-Pd-Pd triplets in $G(r)$ models of the as-quenched and annealed structures. This distribution is much the same as for other metallic glasses, and sharpens

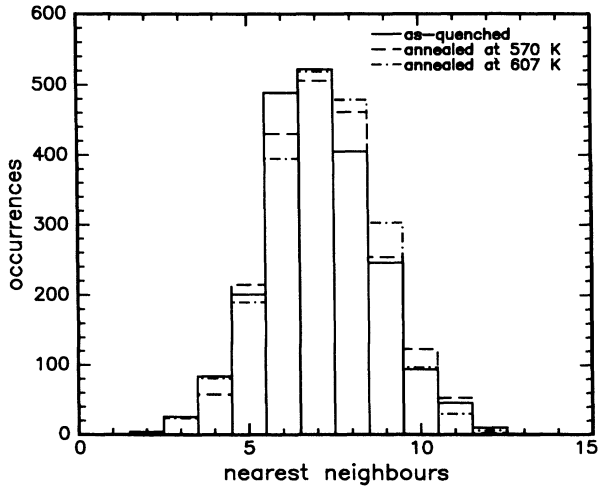

FIG. 8. Nearest-neighbor distribution for Pd atoms in the $G(r)$ models of the as-quenched and annealed states.

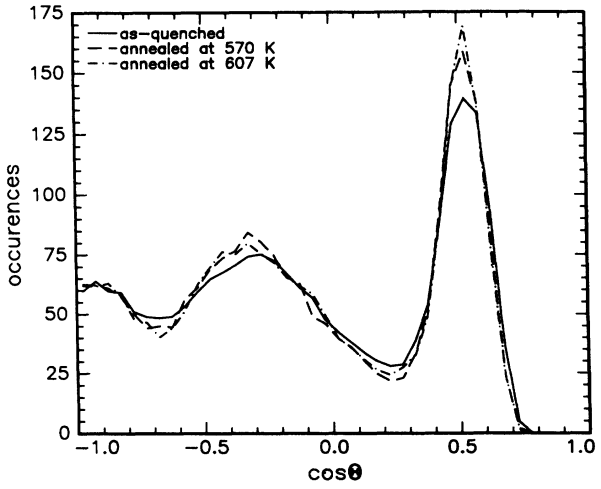

FIG. 9. Cosine distribution of bond angles for Pd triplets in the $G(r)$ models of the as-quenched and annealed states.

upon annealing.[12] It shows that the effect of annealing on the structure (both for annealing at 570 and 607 K) is the increase of the number of Pd triplets with bond angles of 60° or 110° at the cost of triplets with bonds of 80° or 140°. The increase of 60° triplets suggests that annealing *does* affect the nearest-neighbor shell, apparently in a way that does not show a clear effect on the distance distributions. The same results were found for the other models and triplets.

It is interesting to extend the analyses of short-range ordering to other multibody correlation functions and in particular to those who can be compared to interpretations of atomic mobility in metallic glasses. Two candidates are relevant: the nearest-neighbor-shell roughness distribution and the Voronoi volume distribution.

The partial kth-shell roughness of an i-type atom is defined as the variance of the distances of the neighbors of type j,[19]

$$\xi_{ij}^{(k)}=\frac{1}{n_j}\sum_{l=1}^{n_j}(r_{il}-\langle r_{il}\rangle)^2 , \tag{8}$$

with n_j the number of neighbors of type j in the kth shell around the i-type atom under consideration, r_{il} the neighbor distances, and the brackets $\langle\ \rangle$ indicate the average over the n_j neighboring atoms. The nearest-neighbor Pd-Pd roughness distribution (i.e., $k=1$) is given in Fig. 10. Clearly the distribution, which on average involves $n_j\approx 7$ neighboring atoms, sharpens upon annealing, and the annealing treatment at 570 K has the same effect as the treatment at 607 K. Also the *total* roughness distribution, i.e., l counting over *all* neighbors of the central atom, changes in a similar manner. In order to show that the trend observed in the roughness is truly significant, in Fig. 11 the distributions for $\xi_{\text{Pd-Pd}}^{(1)}$ in the different models of the structure of the as-quenched sample and the sample annealed at 570 K are given. It can be seen that, to within the statistical errors, the different models for a particular structure result in the same roughness distribution.

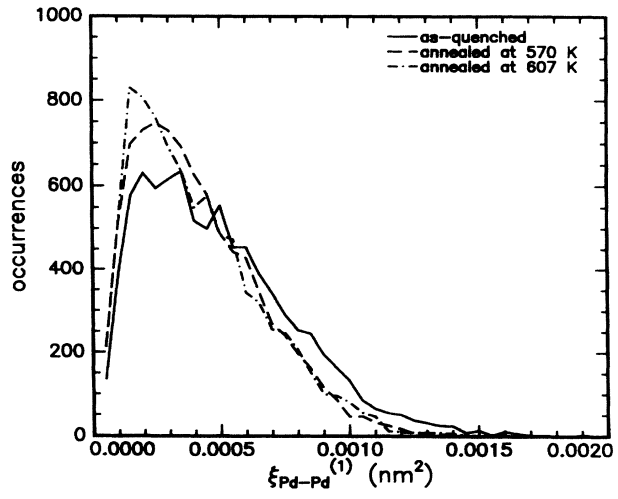

FIG. 10. First-shell roughness distribution for Pd atoms in the models of the as-quenched and annealed states.

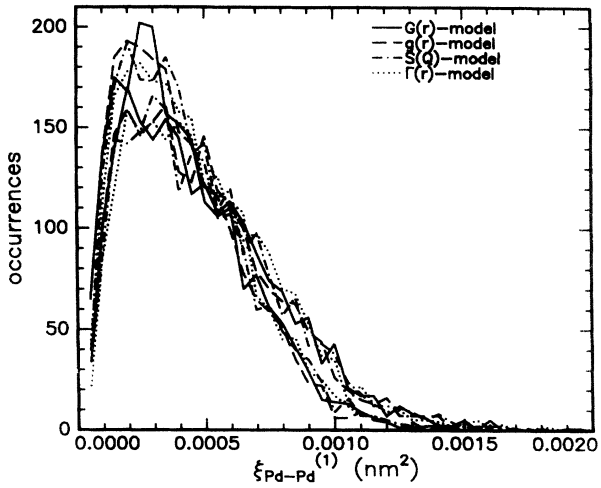

FIG. 11. First-shell roughness distribution calculated for Pd atoms in four different models of the structure of amorphous $Pd_{52}Ni_{32}P_{16}$ in the as-quenched state and after annealing at 570 K.

The above results are consistent with the argument brought forward in Ref. 19 that the number of dissipation sites for vacancies is lower in the annealed than in the as-quenched structures, since sites with high values of ξ collapse more easily than sites with a more spherical shape. This implies that if diffusion in metallic glasses is mediated by vacancies in thermal equilibrium, and if the production sites for these vacancies are the same as the dissipation sites, the present observation implies a lower atomic mobility in the annealed states, in agreement with the experiments.[20]

Another multibody correlation function that can be compared with interpretations of atomic mobility is the Voronoi volume distribution, since this distribution is closely related to the free-volume model of atomic transport in amorphous metals.[21] In the free-volume model, the probability $P(v_f)$ of finding an atom with a Voronoi volume v larger than a critical value v_c, is given by

$$P(v_f)=\frac{p}{\langle v_f\rangle}\exp\left[\frac{-v_f}{\langle v_f\rangle}\right] , \tag{9}$$

with $v_f=v-v_c$ the free volume of a particular atom, v_c is the volume of atoms in the reference structure, where no mobility is possible, $\langle v_f\rangle$ is the average free volume, i.e., the average of $v-v_c$ for $v>v_c$, and p is the fraction of atoms with $v_f>0$. Defects are localized around atoms for which v_f exceeds a critical value v^*. We have calculated the distribution of v by using the so-called radical method for the Voronoi tesselation for a multicomponent system[22] (with $r_{\text{Pd}}=0.140$, $r_{\text{Ni}}=0.125$, and $r_{\text{P}}=0.090$ nm). Figure 12 shows the Voronoi volume distribution of Pd atoms in the models of the as-quenched and annealed structures. The distributions sharpen somewhat upon annealing. A clear effect is found in the tail (upper part of Fig. 12), which is important for atomic mobility. To cal-

culate $\langle v_f \rangle$ we fit Eq. (9) to the high-volume tail of the Voronoi-volume distribution. Systematic deviations from an exponential behavior [Eq. (9)] appear in all three cases at $v \leq 17.6 \times 10^{-3}$ nm^3, leading to the choice $v_c = 17.6 \times 10^{-3}$ nm^3. The average free volume changes from $\langle v_f \rangle = 0.58 \times 10^{-3}$ nm^3 for the as-quenched sample to $\langle v_f \rangle = 0.31 \times 10^{-3}$ nm^3 for the annealed states. For the Ni atoms, the average free volume reduces from $\langle v_f \rangle = 0.49 \times 10^{-3}$ nm^3 to $\langle v_f \rangle = 0.41 \times 10^{-3}$ nm^3, with $v_c = 13.4 \times 10^{-3}$ nm^3. The numbers for the Ni atoms are more uncertain than those for the Pd atoms since the 607 K annealing treatment revealed a systematically smaller effect of annealing on the average free volume for the Ni atoms than the 570 K annealing treatment.

The reduction of the average free volume of roughly 45% for Pd and 15% for Ni is in good agreement with measurements of atomic mobility in amorphous $Pd_{40}Ni_{40}P_{20}$, where a reduction of 25–30% in free volume is found upon annealing.[20] In these experimental studies of atomic mobility $\langle v_f \rangle / v^*$ is determined. The experimental values (as quenched: $\langle v_f \rangle / v^* = 0.04$, annealed $\langle v_f \rangle / v^* = 0.03$) and the present results provide an estimate of v^*, the minimum volume of a defect. For Pd, v^* lies between 10 and 15×10^{-3} nm^3, for Ni between 12 and 13×10^{-3} nm^3, i.e., v^* is a volume that can be looked upon as a vacancy. The consistent behavior of v_c, the good agreement with the experimental study of atomic mobility, and the reasonable size of the Pd and Ni defects give substantial support to the free-volume theory.

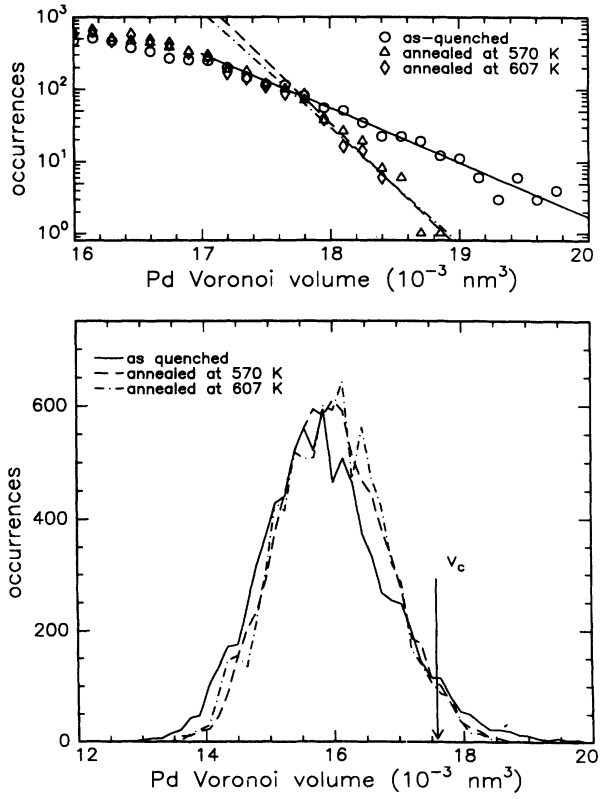

FIG. 12. Voronoi volume distribution for Pd atoms in the models of the as-quenched and annealed states.

B. Medium-range order

Figure 3 shows that the changes in the relative number density $\Delta g(r)$ slightly decrease with increasing r, and it is therefore expected that the effect of annealing on the multibody correlation functions also slightly decreases with increasing r. An example of a multibody correlation function that can be calculated for medium-range distances is given in Fig. 13, where we show the reduced partial radial distribution function of Pd atoms and Pd vertices in $G(r)$ models of as-quenched and annealed states. A vertex is the point where four Voronoi polyhedra meet, i.e., the center of mass of four nearest-neighbor Pd atoms. For a consistent picture, we plot $G_{\text{Pd-vertex}}(r)$ for pair distances larger than the first minimum in $G_{\text{Pd-Pd}}(r)$, since for these distances the correlation is a five-atom correlation. Clearly, there is no effect of annealing, contrary to what is expected from Fig. 3.

There is a small effect of annealing on the roughness of the structure at medium range. This is shown in Fig. 14 where the average roughness of the 4th shell (calculated for atoms between the position of the fourth maximum and the following minimum) is plotted versus the 4th shell Wendt-Abraham parameter $\mathcal{R}^{(4)}$. The relation between the Wendt-Abraham parameter and the average roughness is very weak. Such a weak relation is also found when the second shell roughness and Wendt-Abraham parameter are evaluated, but, as expected, a rather strong relation is found for the nearest-neighbor shell (lower frame of Fig. 14). Apparently, the *qualitative* difference between the effects of annealing on the short-range (peak shift) and medium-range (peak-height increase) pair distances (Fig. 3) is connected to a *quantitative* difference between the effect of annealing on the short-range and medium-range distances for the multibody correlation functions.

The latter point is also illustrated by a set of trial runs to let RMC (although in an unphysical manner) perform the transition from the as-quenched to the annealed structure. Figure 15 shows the result of an RMC simula-

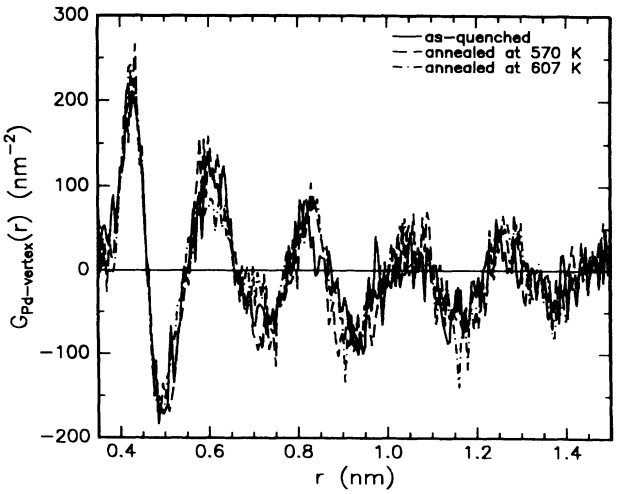

FIG. 13. Calculated partial $G(r)$ for Pd atoms and Pd vertices in the $G(r)$ models of the as-quenched and annealed states.

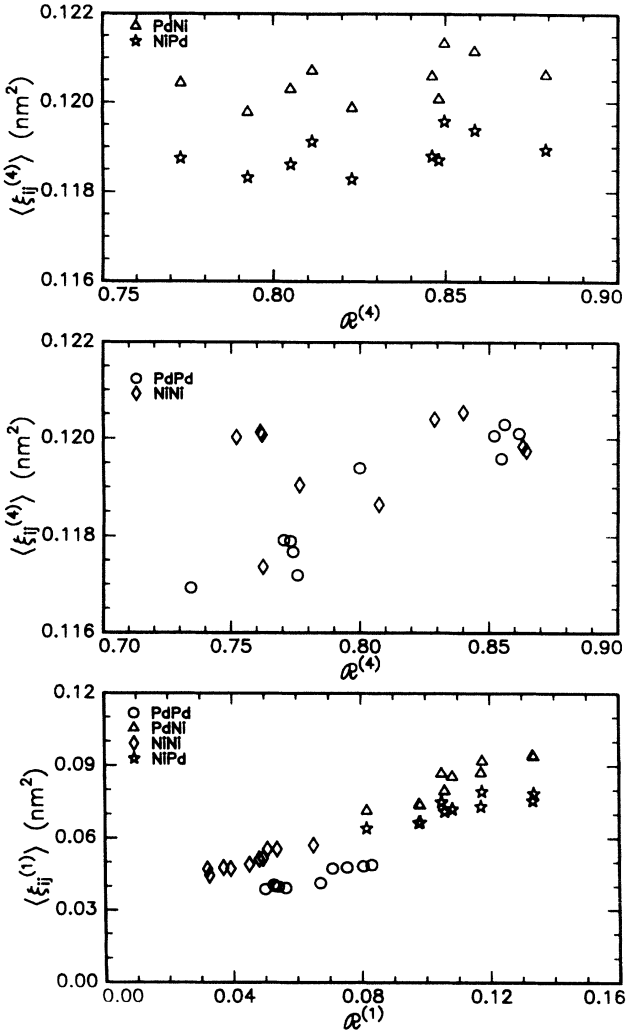

FIG. 14. Upper two panels: Average fourth-shell roughness for metal atoms versus the corresponding Wendt-Abraham parameter $\mathcal{R}^{(4)}$. Lower panel: The same relation for the nearest-neighbor shell.

tion in which the $g(r)$ model for the as-quenched state was taken as the starting configuration and $G^{\rm nat}(r)$, $G^{60}(r)$, and $G^{0}(r)$ for the 570-K state as experimental data. The dotted line in Fig. 15 shows that for $r > 0.6$ nm a good fit could be reached, but for $r < 0.6$ nm the order as present in the as-quenched state could not be significantly changed in the RMC procedure. This indicates that medium-range ordering can occur separately from short-range ordering. In fact, medium-range ordering comes about rather easily (the average displacement per atom from the as-quenched state to the state given by the dotted curve in Fig. 15 is only 0.014 nm) employing random moves of single atoms, but the structural relaxation effects on the short-range order could not be mimicked by moving the atoms one by one.

VI. CONCLUSIONS

The RMC technique has provided models that reflect the changes in the structure of amorphous $Pd_{52}Ni_{32}P_{16}$ upon annealing. The suggested sharpening of the cosine distribution of bond angles, conjectured by Schaal, Lamparter, and Steeb[3] on the basis of a traditional analysis of the radial distribution functions, does indeed appear in these model calculations. Moreover, in addition to these findings, the RMC calculations lend strong support to a reduction of the roughness of nearest-neighbor shells and of a reduction of the free volume in the structure, which is in good agreement with reductions expected on the basis of atomic mobility measurements.

Besides short-range ordering, the medium-range order in the structure of amorphous $Pd_{52}Ni_{32}P_{16}$ increases upon annealing. The diffraction data indicate a qualitative difference between the effect of annealing on the short- and medium-range distances, and the change in the decay rate of the peaks in $G(r)$ suggests that the medium-range order has to be treated as a separate effect of annealing. This conclusion is confirmed by the calculations of multi-

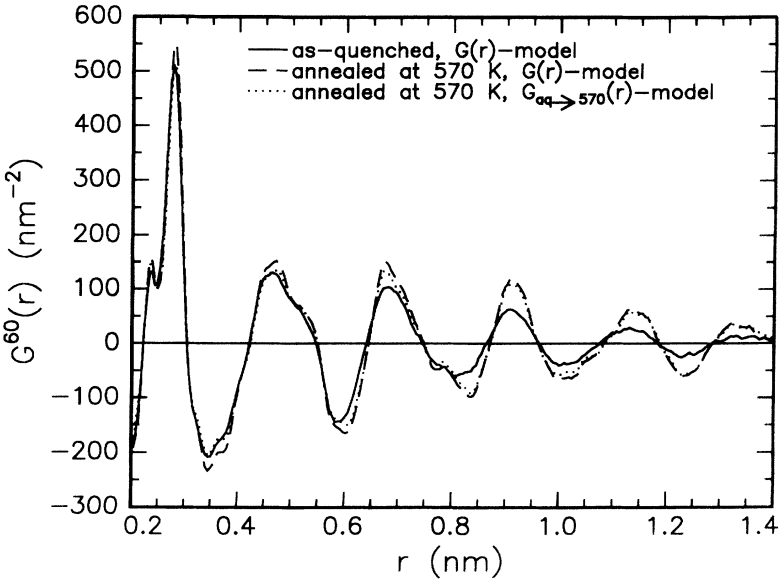

FIG. 15. $G(r)$ models of an as-quenched sample (full line) and a sample annealed at 570 K (dashed line). The dotted line is $G(r)$ for a model obtained by performing RMC on the as-quenched $G(r)$ model, using the radial distribution functions for the 570 K state as input, up to 28 moves per atom.

body correlation functions, which show a quantitative difference between first and higher-order correlations. We therefore suggest that medium-range order is likely not solely brought about by short-range interactions, but has its origin in a change of propagation of order in the structure, and is a separate effect of annealing.

ACKNOWLEDGMENTS

The authors are indebted to Edgar Iparraguirre for cooperation during the initial stages of this investigation, and to Dr. Peter Lamparter (MPI Stuttgart) for providing the data.

[1]D. Srolovitz, T. Egami, and V. Vitek, Phys. Rev. B **24**, 6936 (1981).

[2]R. Brüning and J. O. Ström-Olsen, Phys. Rev. B **41**, 2678 (1990).

[3]M. Schaal, P. Lamparter, and S. Steeb, Z. Naturforsch. Teil A **43**, 1055 (1988).

[4]F. Spaepen, in *Physics of Defects,* Les Houches Lectures XXXV, edited by R. Balian *et al.* (North-Holland, Amsterdam, 1981), p. 135; H. Kronmüller and W. Frank, Radiat. Eff. Defects Solids **108**, 81 (1989); F. Faupel, Phys. Status Solidi A **134**, 9 (1992).

[5]R. L. McGreevy and L. Pusztai, Mol. Simul. **1**, 359 (1988).

[6]L. Pusztai, Z. Naturforsch. Teil A **46**, 69 (1991).

[7]D. A. Keen and R. L. McGreevy, J. Phys. Condens. Matter **3**, 7383 (1991).

[8]E. W. Iparraguirre, J. Sietsma, B. J. Thijsse, and L. Pusztai, Comp. Mater. Sci. **1**, 110 (1993).

[9]L. Pusztai and G. Tóth, J. Chem. Phys. **94**, 3042 (1991); R. L. McGreevy and M. A. Howe, Phys. Chem. Liq. **24**, 1 (1991); B. J. Thijsse and J. Sietsma, in *Proceedings of the 8th International Conference on Rapidly Quenched and Metastable Materials,* Sendai, 1993 [Mater. Sci. Eng. **A179/180**, 438 (1994)].

[10]S. Baer, J. Non-Cryst. Solids **106**, 92 (1988).

[11]B. J. Thijsse and J. Sietsma, in *Proceedings of the 7th International Conference on Liquid and Amorphous Metals,* Kyoto, 1989 [J. Non-Cryst. Solids **117/118**, 176 (1990)].

[12]L. Pusztai, B. J. Thijsse, and J. Sietsma, Philos. Mag. (to be published).

[13]H. R. Wendt and F. F. Abraham, Phys. Rev. Lett. **41**, 1244 (1978).

[14]Schaal *et al.* use, in Ref. 3, the partial coordination numbers of Ni and the changes in the second-neighbor shell of the Ni-Ni partial radial distribution function to make the same point.

[15]R. L. McGreevy, M. A. Howe, and J. D. Wicks, *RMCA Program Manual and Review of the RMC Method* (Oxford University Press, New York, 1993). A copy can be obtained by sending an e-mail request to the authors at: mcgreevy@nflett.sunet.se.

[16]E. W. Iparraguirre, J. Sietsma, and B. J. Thijsse, in *Proceedings of the 8th International Conference on Liquid and Amorphous Metals,* Vienna, 1992 [J. Non-Cryst. Solids **156-158**, 969 (1993)].

[17]P. H. Gaskell, Acta Met. **29**, 1203 (1981).

[18]B. J. Thijsse, J. Appl. Crystallogr. **17**, 61 (1984).

[19]J. M. Delaye and Y. Limoge, in *Proceedings of the 8th International Conference on Liquid and Amorphous Metals,* Vienna, 1992 (Ref. 16), p. 982.

[20]P. A. Duine, J. Sietsma, and A. van den Beukel, Phys. Rev. B **48**, 6957 (1993).

[21]D. Turnbull and M. H. Cohen, J. Chem. Phys. **29**, 1049 (1958); M. H. Cohen and D. Turnbull, *ibid.* **31**, 1164 (1959); **34**, 120 (1961).

[22]B. J. Gellaty and J. L. Finney, J. Non-Cryst. Solids **50**, 313 (1981).